Translational Oncology
www.transonc.com

Volume 6 Number 1 February 2013 pp. 66–74 66

Changes in the Secretory Profile of NSCLC-Associated Fibroblasts after Ablative Radiotherapy: Potential Impact on Angiogenesis and Tumor Growth[1]

Turid Hellevik*, Ingvild Pettersen†, Vivian Berg†, Jack Bruun‡, Kristian Bartnes§, Lill-Tove Busund‡,¶, Anthony Chalmers#, Roy Bremnes*,† and Iñigo Martinez-Zubiaurre†

*Department of Oncology, University Hospital of Northern Norway, Tromsø, Norway; †Department of Clinical Medicine, University of Tromsø, Tromsø, Norway; ‡Department of Medical Biology, University of Tromsø, Tromsø, Norway; §Department of Cardiothoracic and Vascular Surgery, University Hospital of Northern Norway, Tromsø, Norway; ¶Department of Clinical Pathology, University Hospital of Northern Norway, Tromsø, Norway; #Institute of Cancer Sciences, University of Glasgow, Glasgow, UK

Abstract

In the context of radiotherapy, collateral effects of ablative doses of ionizing radiation (AIR) on stromal components of tumors remains understudied. In this work, cancer-associated fibroblasts (CAFs) isolated from freshly resected human lung tumors were exposed to AIR (1× 18 Gy) and analyzed for their release of paracrine factors. Inflammatory mediators and regulators of angiogenesis and tumor growth were analyzed by multiplex protein assays in conditioned medium (CM) from irradiated and non-irradiated CAFs. Additionally, the profile of secreted proteins was examined by proteomics. In functional assays, effects of CAF-CM on proliferative and migratory capacity of lung tumor cells (H-520/H-522) and human umbilical vein endothelial cells (HUVECs) and their tube-forming capacity were assessed. Our data show that exposure of CAFs to AIR results in 1) downregulated release of angiogenic molecules such as stromal cell-derived factor-1, angiopoietin, and thrombospondin-2 (TSP-2); 2) upregulated release of basic fibroblast growth factor from most donors; and 3) unaffected expression levels of hepatocyte growth factor, interleukin-6 (IL-6), IL-8, IL-1β, and tumor necrosis factor–α. CM from irradiated and control CAFs did not affect differently the proliferative or migratory capacity of tumor cells (H-520/H-522), whereas migratory capacity of HUVECs was partially reduced in the presence of irradiated CAF-CM. Overall, we conclude that AIR mediates a transformation on the secretory profile of CAFs that could influence the behavior of other cells in the tumor tissue and hence guide therapeutic outcomes. Downstream consequences of the changes observed in this study merits further investigations.

Translational Oncology (2013) 6, 66–74

Introduction

Non–small cell lung carcinoma (NSCLC) accounts for 80% of all lung cancers, and the combination of high incidence with high mortality rates make NSCLC one of the deadliest cancer types globally [1]. Radiation therapy (RT) continues to be a cornerstone in the treatment of NSCLC, but RT of the thorax is typically limited by the sensitivity of normal lung tissue and the risk of damage to the myocardium. To minimize adverse reactions in healthy tissues, conventional radiotherapy typically consists of daily doses of 2 Gy

Address all correspondence to: Iñigo Martinez-Zubiaurre, PhD, Department of Clinical Medicine, University of Tromsø, N-9037 Tromsø, Norway. E-mail: inigo.martinez@uit.no

[1]This study has been financially supported by grants from the Norwegian Cancer Society and the Northern Norway Regional Health Authority. No competing interests are declared.

Received 12 October 2012; Revised 6 December 2012; Accepted 6 December 2012

DOI 10.1593/tlo.12349

administered over several weeks [2]. However, advances in RT technology now permit accurate delivery of ablative (high) radiation doses to small early-stage tumors in few fractions (<5), with minimal exposure to surrounding normal tissue and therefore acceptable toxicity [3,4]. This novel method of delivering therapeutic ionizing radiation is termed stereotactic ablative radiation therapy (SART). Emerging outcomes from prospective, multi-institutional clinical trials indicate that SART has particular impact on inoperable NSCLC tumors, resulting in considerable improvement of local control and overall survival compared with conventional RT regimens [5,6]. SART in the context of peripheral early-stage inoperable NSCLC is typically delivered in three fractions of 18 Gy [4] and represent a long-sought breakthrough for curative lung cancer therapy [7].

The notion that tumor progression is not restricted to proliferating neoplastic cancer cells, but also relies on the concomitant development of a supportive tumor microenvironment, is now solidified within the scientific community [8–11]. In line with these insights, recent therapy-oriented studies have challenged the view that (high-dose) RT efficacy depends exclusively on direct tumor cell killing, arguing that also indirect regulatory mechanisms emerging from the surrounding stromal components must be taken into consideration [12,13]. One plausible contributing factor to high-dose RT efficacy is the induction of effective immune responses [14,15]. Ablative RT, in contrast to standard RT regimens, reportedly recruits greater numbers of host immune cells into the irradiated tumor volume [16], activates dendritic cells [17], and generates a T cell–dependent immune response that contributes to local tumor reduction and even eradication of distant metastasis in some circumstances [18]. Effects on the tumor vasculature also seems to become evoked by high-dose RT [19], as irradiation of tumor endothelial cells *in vitro* revealed a threshold dose of 1× 10 Gy for induction of apoptosis, with 43% of cells becoming apoptotic after 1× 17 Gy [20].

Cancer-associated fibroblasts (CAFs)—often representing the most abundant cell type of the tumor stroma—is an additional element involved in the regulation of epithelial carcinogenesis [21–24]. Such reactive tumor-resident fibroblasts contribute to cancer development predominantly by the release of paracrine signals that regulate the behavior of other cells in the tumor mass but also stimulate recruitment of endothelial precursor cells [25] and monocytes [26]. Furthermore, CAFs have been nominated as the "leader cell" in the process of collective cancer cell invasion [27], and primary lung tumor CAFs has been found in brain metastases derived from lung carcinoma [28]. Yet, despite the prominent role that fibroblasts play on cancer sustainability, the impact exerted by single high radiation doses (>2 Gy) on tumor-resident fibroblasts is largely unexplored.

In the context of radiotherapy, some groups have shown convincingly that radiation-induced effects in the stromal microenvironment can contribute to malignant progression *in vivo* [29]. In xenograft models, senescent fibroblasts co-transplanted with cancer cells have been found to increase stimulatory effects on cancer growth [30]. Indeed, the transformed phenotype acquired by radiated stromal cells could influence tumor development by the release of senescent cell products, such as matrix metalloproteinases, inflammatory cytokines, or diverse growth factors [31]. Altogether, a growing body of evidences is thus supporting the notion that CAFs may survive radiation exposure, and they are therefore likely to become central players in the regulation of cancer recurrence and resistance to targeted therapies [32–34]. However, it is still unresolved if this phenomenon is tumor type specific or organ specific or whether the senescent phenotype acquired after high-dose radiation exposure is comparable to other forms of senescence [35].

In a recent study from our laboratory, we show that CAFs survive after ablative doses of ionizing radiation (AIR; 1× 18 Gy); however, the cellular phenotype becomes profoundly altered, characterized by the development of senescence and the concomitant induction of growth arrest [36]. We have seen that a single dose of 18 Gy happens to be sublethal for CAFs and that radiation doses above 12 Gy induce enduring DNA damage responses (nuclear foci of 53BP1) and push cells into the permanent senescence stage. Of note, in that study we show that the expression of some matrix metalloproteinases becomes altered along with an overexpression of cell surface integrins, which all together results in a reduction of the migratory and invasive capacity of CAFs. In this preceding study from our group, we describe in detail the isolation and characterization of the NSCLC-derived fibroblast cultures that have been used also for this study. Importantly, flow cytometry analyses using the fibroblast-specific markers α-smooth muscle α-actin and fibroblast activation protein revealed a purity above 99.7%, which gives full credibility to the data generated with this material. This work is intended to complement our initial study on radiation-induced responses by CAFs. Following the rationale of using single high radiation doses to reproduce the effects provoked by SART regimens, in this study we investigate AIR-induced responses mediated by CAFs, with emphasis on paracrine signals that are known to be directly involved in regulation of cancer cell growth and development of tumor vasculature.

Materials and Methods

Human Material, Cell Isolation, and CAF Cultures

Human CAFs were isolated from freshly resected NSCLC tissue specimens, as described previously [36]. Tumors from seven patients not otherwise treated and with an average age of 61 years (range, 51–78) were included in this study. The Regional Ethical Committee approved the study, and all patients provided written informed consent. Fibroblasts from tumors were isolated and characterized following standard procedures. Briefly, tumor resections were collected and cut into 1- to 1.5-mm^3 pieces. Enzymatic digestion of tissues was carried out for 1.5 hours in 10 ml of Dulbecco's modified Eagle's medium/HAM'S F-12 containing bacterial collagenase (Cat. No. C-9407 Sigma-Aldrich, St Louis, MO) at a final concentration of 0.8 mg/ml. Digested tissue was spun for washing and resuspended in fresh growth medium (Dulbecco's modified Eagle's medium/HAM'S F-12 supplemented with 10% FBS). Pure fibroblast cultures were obtained by selective cell detachment from the primary culture mix and by further cell propagation in the presence of 10% FBS. Cells were grown at 3% oxygen and were characterized for purity and cell identity by 1) flow cytometry using fluorescein isothiocyanate–conjugated anti-human α–smooth muscle α-actin antibody (Abcam, Cambridge, United Kingdom; Cat. No. ab8211) [10] and 2) immunofluorescent staining with anti–fibroblast activation protein antibody, a marker for reactive fibroblasts [37].

Cell Lines

Human NSCLC cell lines were cultivated in Nunc EasYFlasks Nunclon Δ (Cat. Nos. 156367 and 156499) in RPMI 1640 medium supplemented with 10% heat deactivated FBS, 4 mM L-glutamine,

and antibiotics. Before the experiments, the cultures were kept in humidified incubators at 37°C with 5% CO_2. Human NSCLC cell lines H522 (Cat. No. NCI-H522 adenocarcinoma) and H520 (Cat. No. NCI-H520 squamous cell carcinoma) were obtained from the American Type Culture Collection (ATCC, Manassas, VA) and cultured as described above. Primary human umbilical cord endothelial cells (HUVECs) were also purchased from ATCC (Cat. No. PCS-100-010). Cell authentication tests and certificates were provided by the manufacturer.

Irradiation of Cells

The intrinsic radioresistance of CAFs in dose-escalating trial experiments have been evaluated and described by us previously [36]. Briefly, adherent CAFs cultured in flasks were irradiated with high-energy photons produced by a Varian clinical linear accelerator, delivered as single doses of 2, 6, 12, and 18 Gy or after fractionated 6× 3 Gy. Standard parameters for dose delivery were depth of 30 mm, beam quality of 15 MV, dose rate of 6 Gy/min, and field size of 20 × 20 cm. Radiation doses were confirmed by thermoluminescent dosimeters. Cell death after radiation was assessed by xCELLigence and by light microscopy for 3 weeks after radiation exposure. Standard assays to test viability such as 3-(4,5-dimethylthiazol-2-yl)-2,5-diphenyltetrazolium bromide (MTT) and clonogenic survival could not be used in our CAF culture system because the differences observed after long incubation periods between irradiated and non-irradiated cells were a consequence of premature cell senescence rather than cell death.

Preparation of Conditioned Medium

CAF cultures were established from five randomly selected and untreated donors and grown in T75 culture flasks at low oxygen (3%), followed by irradiation (1× 18 Gy) of semiconfluent cells. Culture medium from irradiated and control CAFs was collected between days 4 and 6 post-irradiation. Supernatants were spun down and filtered for elimination of potential contaminant cell bodies. Finally, the collected medium was concentrated in VIVASPIN (3000-MW cutoff size).

Fluorescent Bead-Based Fluorokine Multianalyte Profiling Assay (Luminex; Bio-Rad, Hercules, CA)

Quantitative measurements of cytokines and growth factors were performed using a suspension array technique (Bio-Plex 200; Bio-Rad) [38,39]. CAF–conditioned medium (CM) from five randomly selected donors was prepared as indicated previously. Protein levels of inflammatory factors [tumor necrosis factor–α (TNF-α), interleukin-1β (IL-1β), IL-6, and IL-8] and growth factors [hepatocyte growth factor (HGF), basic fibroblast growth factor (bFGF), platelet-derived growth factor (PDGF), and vascular endothelial growth factor (VEGF)] were analyzed in a cytokine multiplex panel (Cat. No. 171B5026M, Bio-Rad), and angiogenic factors were examined with a multiplex panel (Cat. No. LAN1635, LAN265, LAN 923; R&D Systems, Abingdon, United Kingdom). All samples were analyzed in duplicates and in dilutions of 1:4. Levels of proteins included in the arrays were detected using the Bio-Plex 200 analyzer, according to instructions from the manufacturer. Data were processed using SPSS statistical software version 16.0 (SPSS Inc, Chicago, IL). The secretion levels were examined for statistical significance using the Wilcoxon signed-rank test. Only readings above the detection limit of the assay are represented in figures. The values are expressed as mean ± SEM. A P value < .05 denoted the presence of a statistically significant difference.

Analyses of the Secretome by Proteomics and Exponentially Modified Protein Abundance Index Calculation

CAF supernatants from irradiated and non-irradiated cells were collected between days 4 to 6 post-treatment, concentrated in VIVASPIN (3000-MW cutoff) centrifuge tubes, and run in one-dimensional sodium dodecyl sulfate–polyacrylamide gel electrophoresis. Upon staining of gels with Coomassie blue, the entire band spectrum in the gels from each supernatant was excised into 24 gel fractions. After excision, gel bands were subjected to in-gel reduction, alkylation, and digestion using 2 to 10 ng/μl trypsin (V511A; Promega, Madison, CA) [40]. Peptide mixtures containing 0.1% formic acid were loaded onto a nanoACQUITY UltraPerformance LC (Waters, Milford, MA), containing a 3-μm Symmetry C18 Trap column (180 μm × 22 mm; Waters) in front of a 1.7-μm BEH130 C18 analytical column (100 μm × 100 mm; Waters). Peptides were separated with a gradient of 5% to 95% acetonitrile and 0.1% formic acid, with a flow of 0.4 μl/min eluted to a Q-TOF Ultima mass spectrometer (Micromass/Waters). Samples were run in data-dependent tandem mass spectrometry (MS) mode. The relative abundance of proteins was calculated using the Exponentially Modified Protein Abundance Index (emPAI) [41]. Briefly, peak lists were generated from MS/MS by Mascot Distiller 2.3.2 (Matrix Sciences, Boston, MA). All raw data files from one patient were merged into one mascot generic file (MGF) peak list. The resulting MGF files were searched against the Swiss-Prot 57.15 protein sequence databases using an in-house Mascot 2.3 server (Matrix Sciences). Peptide mass tolerances used in the search were 100 ppm, and fragment mass tolerance was 0.1 Da. The emPAI was collected from the mascot results for each protein ID.

Real-Time Monitoring of Cell Growth in xCELLigence E-plates

Proliferation rates were monitored continuously by exploiting the xCELLigence System from Roche Applied Sciences (Indianapolis, IN), consisting of microtiter E-plates with gold microarrays integrated in bottom of wells and the RTCA-DP instrument for plate readouts, previously described by us [36] and others [42–44] . Briefly, tumor cells (H520 and H522) and endothelial cells (HUVECs) were seeded in E-plates at densities of 10,000 and 5000 cells/well, respectively. Upon attachment (initial 3 hours), cells received (1:1) volumes of CAF-CM) from irradiated and non-irradiated cells prepared from three different donors. Automated real-time monitoring of E-plates was performed by the RTCA-DP instrument at standard incubator conditions, with triplicate readouts of the dimensionless parameter cell index every 30 minutes during the following 7 days.

Real-Time Monitoring of Cellular Migration in xCELLigence CIM Plates

Onset and rate of migration was monitored continuously by exploiting the Cell-Invasion-and-Migration (CIM) plates corresponding to the xCELLigence System, described previously [36,45]. In this study, migration assays were performed as follows: Tumor cells (H520 and H522) and endothelial cells (HUVECs) were seeded in the upper chamber of CIM plates at densities of 50,000 cells/well for tumor cell lines (H520 and H522) and 30,000 cells/well for endothelial cells. The lower and upper chambers of the CIM plates were filled with 1:1 dilution of CAF-CM mixed with each cell line–specific growing medium. Upon equilibration (1-hour incubation at room temperature), CIM plates were transferred into the RTCA DP instrument for readouts every 15 minutes during 48 hours. Impedance (cell index) was registered only from cells capable of migrating through the 8-μm

porous membrane, and readout was performed in three parallel wells per condition.

In Vitro *Tubule Forming Assay*

The formation of capillary-like structures was assessed in Matrigel-coated multiwell plates essentially as described [46]. HUVECs at early passages were collected and seeded at a density of 5×10^4 cells/well in 24-well plates coated with 230 µl of Matrigel (BD, Cat. No. 356231). Cell attachment was allowed during the initial 2 hours at 37°C and from then on HUVECs were exposed to CAF-CM mixed in a 1:1 proportion with serum-free HUVEC medium. Incubation was carried out for 20 hours thereafter. Formation of tubular structures was examined with a Nikon Eclipse TS100 model light microscope. Randomly selected fields were photographed at ×40 magnification, using an Idea SPOT digital camera. Capillary-like tubular structures were scored by counting the number of tubules in each well (numbers were extrapolated from counting three randomly selected microscope fields per well). Data are the means ± SD from three independent experiments, each performed in duplicates.

Results

Secretion of Paracrine Factors Regulating Tumor Growth, Inflammation, and Angiogenesis

CAFs are thought to exert most of their tumor promoting functions through expression of paracrine molecules that either directly stimulates growth of cancer cells or influence growth and functions of other cells from the tumor stroma. Thus, we studied the impact of AIR (1× 18 Gy) on expression of a panel of factors known to be important regulators of inflammation, angiogenesis, or tumor growth, using antibody-based multiplex protein arrays in supernatants derived from reactive CAF cultures from various donors. Our results show that while a number of major inflammatory/immune mediators such as IL-6 and IL-8 and also TNF-α are readily produced by CAFs, secretion of these factors is not modified by AIR (Figure 1*A*). Another important immunoregulator, IL-1β, was not detected in CAF–culture supernatants (not shown). In the case of angiogenic regulators, CAFs expressed all five factors included in the array (Figure 1*B*). Of these, AIR caused a significant reduction ($P < .05$) in expression of stromal cell-derived factor-1α (SDF-1α), angiopoietin-1 (ANG-1), and TSP-2. Among the various growth factors studied, HGF and, to a lesser extent, bFGF were produced by CAFs, whereas PDGF was not detected (Figure 1*C*). Interestingly, a potent induction of bFGF (~10 fold in some donors) was observed in irradiated CAFs from four out of five donors, whereas secretion of the other studied growth factors was not changed.

Proteomic Analyses of the CAF Secretome after AIR

To undertake an unbiased assessment and to search for novel or alternative paracrine signals released by CAFs that may influence tumor development, the entire secretome was analyzed by proteomics and the relative abundance of detected proteins estimated using the emPAI. On average, a total of 135 proteins with acceptable mascot scores were identified in supernatants of non-irradiated cells and 181 proteins in supernatants of irradiated cells. Identified proteins were classified by functionality (data not shown). The most abundantly expressed protein types were matrix components and

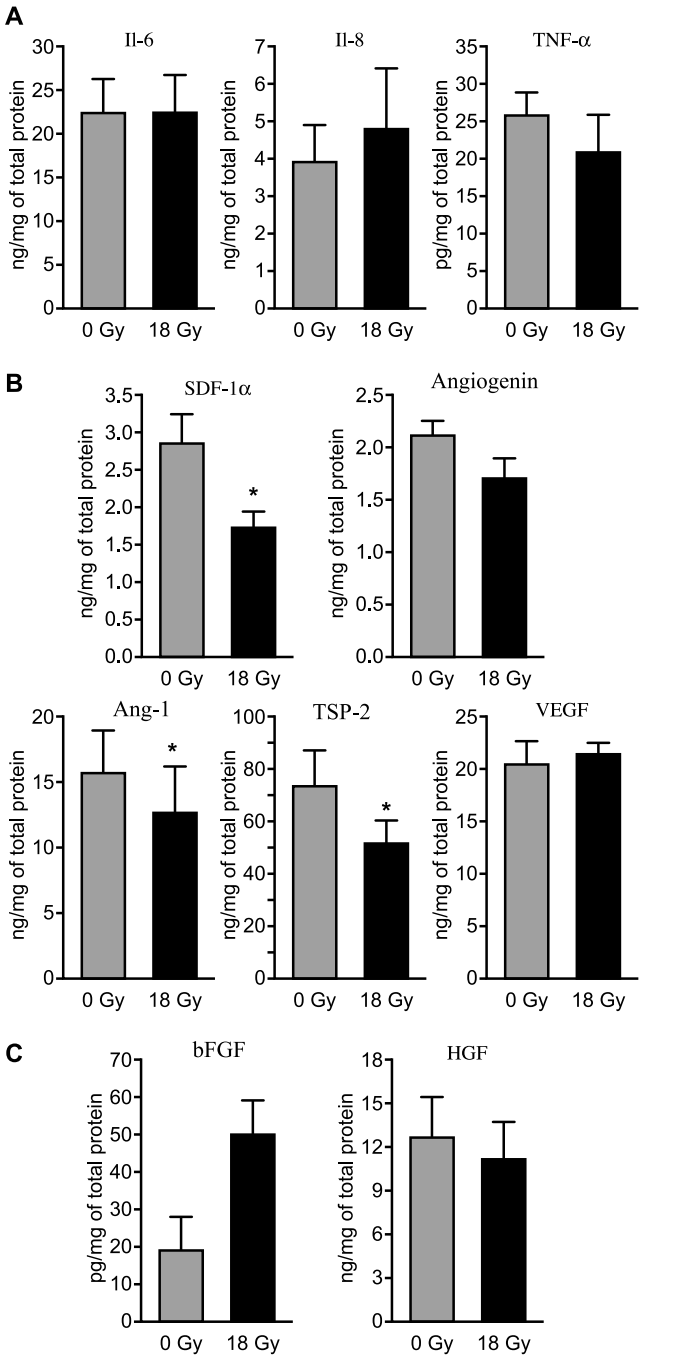

Figure 1. Secretion of tumor regulatory molecules by irradiated and non-irradiated CAFs. Quantitative determinations of growth factors and cytokines in culture supernatants from five different donors were measured by multiplex protein arrays. Only factors giving values above the detection limit of the assay are represented. Panel (A) demonstrates expression of inflammatory molecules. The following cytokines were included in the array: IL-1β, IL-6, IL-8, and TNF-α. Panel (B) shows array of angiogenic factors including SDF-1α, angiogenin, angiopoietin, TSP-2, and VEGF. Finally, (C) presents array of detectable tumor growth regulators, comprising HGF, bFGF, and PDGF. Mean values from five different donor samples are shown; statistical analyses were performed by applying paired samples Student's *t* test. Statistically significant differences are indicated by asterisk ($P < .05$).

Table 1. List of Tumor Regulatory Agents Identified in CAF Supernatants by Proteomics.

Protein Name	Positive ID*	Protein Acronym†	Mascot Score	Protein Cover	emPAI 0 Gy	emPAI 18 Gy	Fold Change 0 *versus* 18 Gy
Pigment epithelium–derived factor	$n = 4$	PEDF	319	34.7	0.59 (±0.3)	0.15 (±0.1)	↓ 3.9
Thrombospondin-1	$n = 5$	TSP-1	434	17.6	0.46 (±0.3)	0.33 (±0.1)	↓ 1.4
Thrombospondin-2	$n = 2$	TSP-2	233	7.7	0.10 (±0.06)	0.07 (±0.1)	↓ 1.4
Insulin-like growth factor 2	$n = 1$	IGF-2	59	6.1	–	0.19	–
Growth arrest-specific protein 6	$n = 4$	GAS-6	363	18.3	0.13 (±0.1)	0.25 (±0.2)	↑ 1.9
Macrophage migratory inhibitory factor	$n = 2$	MIF	77	17.4	0.15 (±0.2)	0.51 (±0.2)	↑ 3.4
Connective tissue growth factor	$n = 2$	CTGF	47	4.8	0.14 (±0.07)	0.04 (±0.0)	↓ 3.5
Interleukin-6	$n = 2$	IL-6	158	22.2	0.48 (±0.4)	0.17 (±0.2)	↓ 2.8

emPAI: Average values from positive determinations.
*Number of donors in which the protein was identified from a total of five analyzed.
†Human.

matrix regulatory molecules. Other protein types included metabolic enzymes, binding proteins, and inhibitory or stimulatory growth factors. Regarding inflammatory mediators, angiogenic factors, and tumor growth regulators, only eight relevant factors could be identified in all or some of the donors (Table 1). In line with the data generated by multiplex protein arrays, we observed a reduction (approximately 1.4-fold) in the expression of angiogenic regulators such as TSP-1 and TSP-2 after applying semiquantitative determinations to compare irradiated and non-irradiated CAFs. Expression of the inflammatory mediator IL-6 was found to be reduced in the supernatants in which it was detected (2.8-fold), whereas expression of macrophage migratory inhibitory factor was enhanced (3.4-fold). Other tumor growth regulators modified by AIR were insulin-like growth factor 2 (IGF-2; not detected on 0 Gy), connective tissue growth factor (CTGF; 3.5-fold downregulated), and growth arrest-specific protein 6 (GAS-6; 1.9-fold upregulated).

Effects of Secreted Molecules on the Proliferative and Migratory Capacity of Lung Neoplastic Cells

To determine if secreted factors from irradiated and/or non-irradiated CAFs influenced the proliferative and invasive capacity of epithelial tumor cells, H520 lung squamous carcinoma cells and H522 lung adenocarcinoma cells were exposed to CAF-CM isolated from different random donors. Proliferation of tumor cells was monitored continuously over a 1-week period on E-plates. Results showed no influence of CAF-CM on the proliferation rate of either H520 (Figure 2*A*) or H522 tumor cells (Figure 2*B*). Similar outcomes were observed after using fibroblast CM prepared from three different

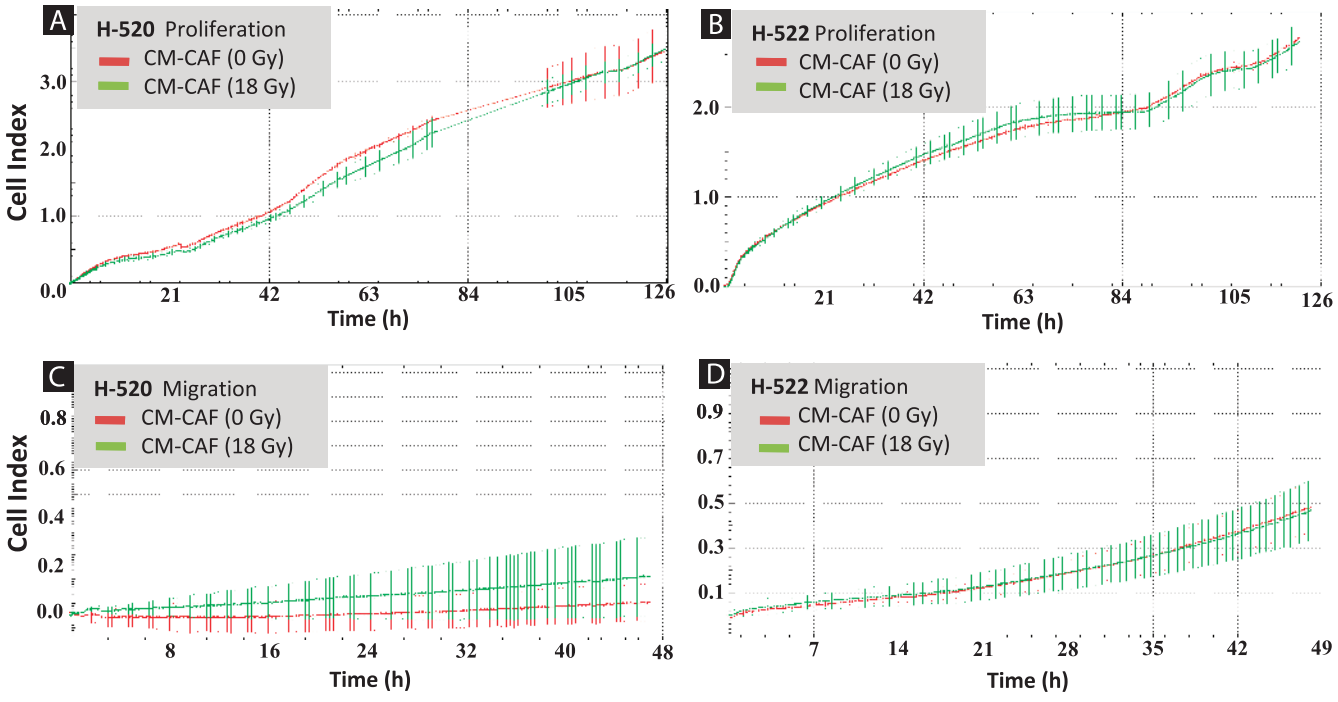

Figure 2. Effect of CAF-CM on proliferative and migratory capacity of lung tumor cell lines H520 and H522. CAFs cultured in T-75 flasks were treated with 1× 18 Gy and medium was conditioned in a serum-free setting for 4 to 6 days post-irradiation. Proliferative capacity of two lung carcinoma cell lines, H520 (squamous cell carcinoma) (A) and H522 (adenocarcinoma) (B), was monitored on E-plates located in the xCELLigence machine, whereas corresponding migratory capacity of H520 and H522 in double-chambered CIM plates is presented in (C) and (D), respectively. For both experiments, H520 and H522 were exposed to (1:1) non-irradiated CAF-CM (red line) and (1:1) irradiated CAF-CM (green line) from a randomly selected donor. Similar profiles were obtained after running the assay with CAF-CM from three different donors.

donors (data not shown). In a different set of experiments, the migratory capacity of H520 (Figure 2*C*) and H522 tumor cells (Figure 2*D*) was compared in the presence of CAF-CM from irradiated (18 Gy) or non-irradiated (0 Gy) CAFs over a 48-hour period. Using this system, migration of H520 cells was nearly undetectable, and changes in migration rates could not be measured. However, H522 cells migrated efficiently, but CAF-CM did not significantly affect this behavior.

Effects of Secreted Molecules on the Proliferative and Migratory Capacity of Endothelial Cells (HUVECs)

To determine if secreted factors from irradiated and non-irradiated CAFs had influence on the proliferative and migratory capacity of endothelial cells, HUVECs were exposed to CAF-CM isolated from three different donors. Proliferation of HUVECs was monitored continuously over 1 week on E-plates by the xCELLigence System. The results showed that 1) HUVECs lose their proliferative capacity in the absence of serum (seen as flattening of cell index values) and 2) CM from irradiated and non-irradiated CAFs had no influence on the proliferation rates of HUVECs (Figure 3*A*). Similar outcomes were observed with CAF-CM from three different donors (data not shown). Regarding migration, unlike for tumor cell lines, CAF-CM was essential to promote migration of HUVECs in the absence of serum. Interestingly, CAF-CM from irradiated cells resulted in a considerable reduction of the migratory capacity of HUVECs when compared to CAF-CM from non-irradiated cells (Figure 3*B*). Migratory activity of HUVECs exposed to CM from irradiated CAFs (CAF-CM 18 Gy) was on average 26% lower than for HUVECs exposed to CM from non-irradiated CAFs, when calculating cell index values after 20 hours of observation in CIM plates (Figure 3*C*). For the quantitative data (Figure 3*C*), CI values reflect average numbers from seven independent experiments and readouts by the xCELLigence System, using CAF-CM from seven randomly selected donors. Nevertheless, statistical analyses with this number of donors using Wilcoxon signed-rank test revealed $P = .06$.

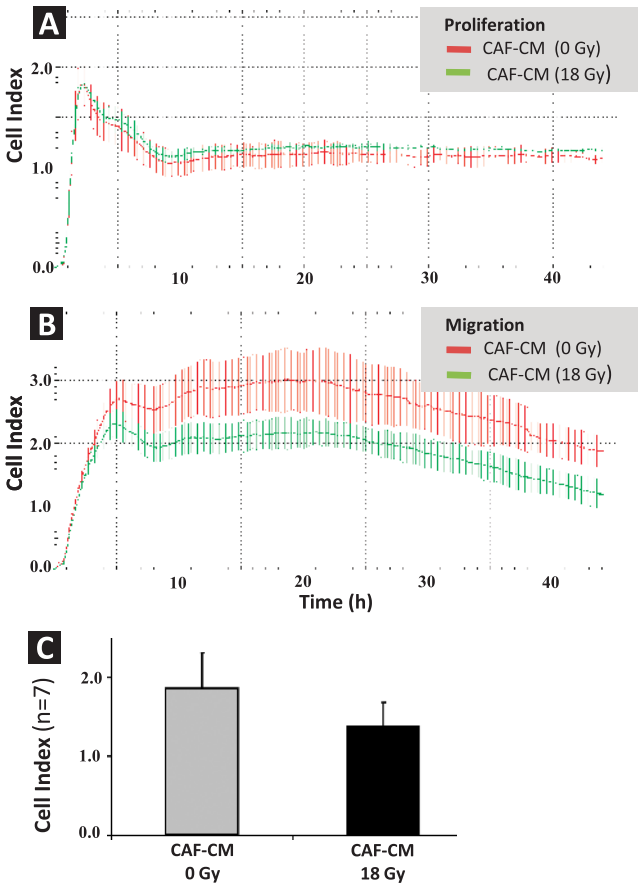

Figure 3. Effect of CAF-CM on the proliferative and migratory capacity of HUVECs. CAFs were treated with 1× 18 Gy and incubation medium was conditioned in serum-free conditions for 4 to 6 days post-irradiation. Proliferative capacity of HUVECs was monitored on E-plates (A) and migratory capacity in double-chambered CIM plates (B), with readout by the xCELLigence System for both types of plates. For both experiments, HUVECs were exposed to (1:1) non-irradiated CAF-CM (red line), and (1:1) 1× 18 Gy irradiated CAF-CM (green line) from one randomly selected donor. Similar profiles were obtained after running the assay with CAF-CM from seven different donors. Columns in (C) represent mean and SEs of CI values after a 20-hour observation of HUVEC migratory behavior, averaged from seven independent experiments using CAF-CM from seven randomly selected donors. Error bars represent SD.

Effects of Secreted Molecules on Endothelial Cell Tube Formation

To further investigate the effects of CAF-released paracrine signals on endothelial cell behavior, we performed *endothelial cell tube formation assays* in the presence of CAF-CM. This widely used *in vitro* angiogenesis assay intends to visualize and quantify formation of capillary structures in a basement membrane matrix, hence allowing scientists to explore compounds that promotes or inhibits angiogenesis. Using this assay, we found that HUVECs grown in the presence of standard HUVEC incubation media do indeed make tubes (Figure 4*A*) but with a much lower quantity and quality than HUVECs exposed to CAF-CM (Figure 4*B*), i.e., 417 *versus* 721 tubes/well, respectively. Tube-forming capacity of HUVECs exposed to CM from non-irradiated *versus* irradiated CAFs demonstrated similar morphology and also similar numbers in respect to tube formation, 721 *versus* 672 tubes/well, respectively (Figure 4*C*).

Discussion

In this study, we have mapped the CAF-mediated release of signaling molecules implicated in inflammation, angiogenesis, and tumor growth and have examined the impact of such radiation-induced disturbances on growth and proliferation of tumor cells and endothelial cells. Our results show that important tumor-regulatory molecules released by CAFs are differentially regulated after exposure to AIR. Of note, a number of angiogenic factors including SDF-1, angiopoietin, and TSP-1 are downregulated, whereas molecules such as bFGF are upregulated. In functional assays with lung tumor cell lines and endothelial cells we have not observed considerable changes in the growth or migratory properties of cells, besides the moderate downregulated migration of HUVECs exposed to irradiated CAF-CM. Although in our experimental system the pull of released factors from CAF was not able to induce significant regulation of the mentioned cell functions, an altered secretion of signal molecules upon AIR does occur and warrant close attention.

In a recently published work, we reported that after exposure to a single radiation dose of 18 Gy, CAFs develop a senescent phenotype with reduced migratory and invasive capacities, and these phenomena were

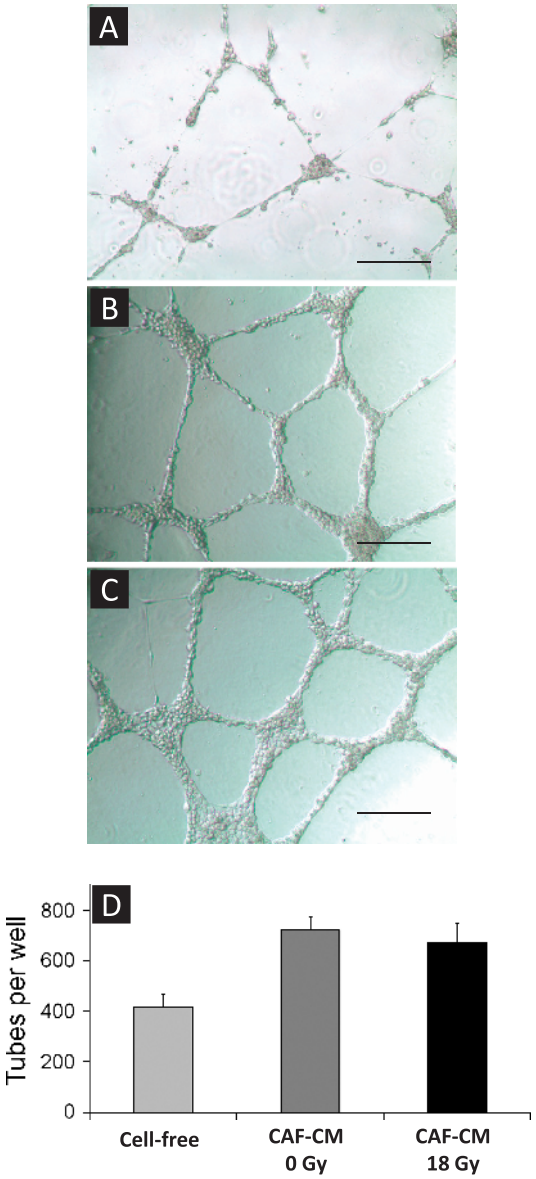

Figure 4. Effect of CAF-CM on endothelial cell tube formation. CAFs were treated with 1× 18 Gy and incubation medium was conditioned in serum-free conditions between days 4 and 6 post-irradiation. HUVECs were plated in Matrigel-coated multiwell plates, and after an attachment phase of 2 hours, HUVECs were exposed to CM from irradiated (18 Gy) and non-irradiated CAFs (0 Gy) and incubated for another 20 hours. Images show tube formation by HUVECs after 20 hours of growth in Matrigel. In (A), tube formation by HUVECs exposed to standard (cell-free) incubation medium is shown, whereas (B) and (C) demonstrate tube-forming HUVECs exposed to CM from non-irradiated CAFs (CAF-CM 0 Gy) and irradiated CAFs (CAF-CM 18 Gy), respectively. Bars, 320 μm. Panel (D) reflects quantification of HUVEC forming tubes/well. Data represent average values from three independent experiments (error bars represent SD).

attributable to stabilization and redistribution of focal contacts within the plasma membrane [36]. In that study, we also showed that expression of matrix-degrading enzymes such as matrix metalloproteinase-1 is downregulated (in four out of five donors) after AIR. Other laboratories have also shown that ionizing radiation can provoke a senescence-like phenotype in fibroblasts receiving a single dose of 10 Gy [31]. Previous reports argue that after both replicative senescence [47] and stress-induced senescence, fibroblasts (cell lines) and malignant cells acquire an activated phenotype characterized by increased production of proteolytic enzymes, cytokines, growth factors, and reactive oxygen species that promote tumor growth and survival [30,31,47–49]. However, the overall tumor regulatory properties of senescent fibroblasts remain controversial. Some authors have suggested that cancer promotion by *senescent* stromal cells may be restricted to certain organ and tissue types and claim that the importance of senescent cells needs to be validated in other sites than subcutaneously grown tumors [35].

Activated fibroblasts undeniably represent an important source of cytokines and immunomodulators that influence the inflammatory process during tumor development [10,23,50]. Our data confirm that reactive lung CAFs indeed produce cytokines such as IL-6, IL-8, and TNF-α, whereas molecules such as IL-1β were below the limits of detection. Hanahan et al. have demonstrated, similarly to us, that CAFs from skin, breast, or pancreatic cancers possess a pro-inflammatory gene signature that is already activated in CAFs before irradiation, including upregulated levels of IL-6 in CAFs *versus* normal fibroblasts as well as low levels of IL-1β [51]. In accordance with another study [52], we observed that AIR do not alter significantly the production of any of these cytokines in CAFs. On the opposite, others have shown that large single radiation doses (10 Gy) induce senescence in (diploid) fibroblasts and that this phenotype is featured by a marked induction of IL-6 and IL-8 production that could promote tumor progression [31]. These discrepancies may be attributed to the differences in the experimental models used. We are one of few groups using freshly isolated CAFs from tumor specimens derived from multiple donors. Other laboratories are using long-passage cell lines derived initially from normal tissue fibroblasts, displaying phenotypes that may have been altered by prolonged culturing. For a proper interpretation of results, the activated nature of tumor-resident fibroblasts has to be taken into consideration.

In this study, we have also explored the secretion of CAF-derived growth factors that may exert a direct impact on tumor growth [53] as well as resistance to molecularly targeted therapies [54]. Our data show that some recognized growth factor molecules, such as HGF and to a lesser extent bFGF, are secreted by NSCLC-derived CAFs. After exposure to AIR, secreted bFGF levels from CAFs were noticeably enhanced, whereas HGF levels were unchanged. These findings are in agreement with results achieved by exposing stromal fibroblasts from pancreatic cancer to 1× 10 Gy [53]. Notably, fibroblast growth factor-2 (or bFGF) is reported to mediate radioprotective effects on the tumor vasculature [55] and also function as an independent negative predictor of local tumor control and overall survival for patients irradiated for stage II to III NSCLC [56]. However, recent studies have demonstrated HGF-induced resistance to anti-tumoral effects mediated by epidermal growth factor receptor–tyrosine kinase inhibitors in lung cancer [32], triple-negative breast cancer [33], and also BRAF-mutant melanomas [34,57]. Accordingly; inhibition of HGF activity has demonstrated enhanced therapeutic responses in lung [58] and pancreatic cancers [53]. PDGF, a relevant tumor regulatory molecule that can be expressed by tumor fibroblasts, was not detected in NSCLC-CAF supernatants by us. These contradictory observations could be explained by tissue-specific patterns of secretion from CAFs of different tumor types.

In our unbiased proteomic approach, we could detect expression of other important tumor growth regulators such as IGF-2, CTGF,

GAS-6, and pigment epithelium–derived factor (PEDF). Semiquantitative determinations show that while the expression of the pro-tumorigenic macrophage migration inhibitory factor [59] and the senescent marker GAS-6 were enhanced upon radiation, expression of the matrix regulatory molecule CTGF and the anti-tumorigenic factor PEDF were reduced. Notably, it has been recently suggested that metabolically reprogrammed and CTGF-overexpressing CAFs are mediating growth of breast cancer cells, without a concomitant increase in angiogenesis [60]. Results from our functional studies, using H522 adenocarcinoma and H520 squamous cell carcinoma cell lines derived from NSCLC, did not reveal any perturbation of the proliferative or migratory capacity of tumor cells exposed to CAF-CM. This may indicate that the observed changes in the secretory profile of CAFs upon AIR do not exert a measurable impact on the adjacent lung tumor cells. However, it should be kept in mind that our functional assays were performed on cell lines in cell culture conditions that may or may not represent the behavior of lung carcinoma cells *in vivo*.

Moreover, we have explored the CAF-mediated effects of AIR on the expression of major regulators of angiogenesis. The role of CAFs as providers of pro-angiogenic factors is well documented [10,25]. Indeed, in many instances, angiogenic inducers expressed within tumors are produced in higher quantities by stromal cells than by the tumor cells themselves [61]. Importantly, the secretion of SDF-1 by CAFs enhances the recruitment of endothelial progenitor cells into the tumor neovasculature, thereby promoting neovasculogenesis [25,62] and eventually tumor recurrence. To our knowledge, regulation of the angiogenic response by irradiated CAFs has not been documented hitherto. Our data show that VEGF is abundantly expressed by CAFs, but its expression is not consistently modified by AIR. However, production of factors such as angiopoietin and SDF-1 was significantly reduced in irradiated CAFs, along with a reduction of the anti-angiogenic factor TSP-2. In line with the results obtained by multiplex protein assays, TSP-1 and TSP-2 were found to be downregulated by AIR in our proteomic analyzes. To investigate the relevance of these findings, we performed functional assays that demonstrated that, while the proliferative capacity of endothelial cells was unaltered after exposure to CM from irradiated CAFs, their migratory capacity was reduced. In tube-forming assays, endothelial cells were showing dependence on CAF-CM to form stable capillary-like structures in serum-free conditions; however, irradiation of CAFs did not introduce measurable differences in this functional assay. Our study did not include *in vivo* measurements of the recruitment of endothelial progenitors, but taken together our data support the notion that exposure of CAFs to high radiation doses causes a significant reduction in some of their pro-angiogenic properties. This conclusion does not rule out the possibility that radiation might induce pro-angiogenic effects through tumor components other than CAFs.

Conclusions

Central paracrine molecules released by CAFs that are implicated in overall tumor sustainability are differentially regulated upon AIR. Thus, whereas the expression of a number of major inflammatory mediators remains unchanged, growth factors such as bFGF are upregulated. In addition, the CAF-mediated angiogenic response appears to be inhibited by AIR: The migratory capacity of endothelial cells is reduced in the presence of CM from irradiated CAFs, and the expression of angiogenic inducers such as angiopoietin and SDF-1 is significantly reduced. Overall, our results suggest that some of the beneficial therapeutic effects of AIR could be linked to a reduction of the tumor promoting properties of CAFs, but the overall impact of such disturbances *in vivo* remains to be studied.

Acknowledgments

The technical assistance with the figures by Rod Wolstenholme is highly appreciated.

References

[1] Ferlay J, Shin HR, Bray F, Forman D, Mathers C, and Parkin DM (2010). Estimates of worldwide burden of cancer in 2008: GLOBOCAN 2008. *Int J Cancer* **127**, 2893–2917.

[2] Powell JW, Dexter E, Scalzetti EM, and Bogart JA (2009). Treatment advances for medically inoperable non-small-cell lung cancer: emphasis on prospective trials. *Lancet Oncol* **10**, 885–894.

[3] Kavanagh BD, Miften M, and Rabinovitch RA (2011). Advances in treatment techniques: stereotactic body radiation therapy and the spread of hypofractionation. *Cancer J* **17**, 177–181.

[4] Heinzerling JH, Kavanagh B, and Timmerman RD (2011). Stereotactic ablative radiation therapy for primary lung tumors. *Cancer J* **17**, 28–32.

[5] Lanni TB Jr, Grills IS, Kestin LL, and Robertson JM (2011). Stereotactic radiotherapy reduces treatment cost while improving overall survival and local control over standard fractionated radiation therapy for medically inoperable non-small-cell lung cancer. *Am J Clin Oncol* **34**, 494–498.

[6] Palma D and Senan S (2011). Stereotactic radiation therapy: changing treatment paradigms for stage I nonsmall cell lung cancer. *Curr Opin Oncol* **23**, 133–139.

[7] Senan S, Palma DA, and Lagerwaard FJ (2011). Stereotactic ablative radiotherapy for stage I NSCLC: recent advances and controversies. *J Thorac Dis* **3**, 189–196.

[8] Hanahan D and Weinberg RA (2000). The hallmarks of cancer. *Cell* **100**, 57–70.

[9] Bissell MJ and Radisky D (2001). Putting tumours in context. *Nat Rev Cancer* **1**, 46–54.

[10] Hanahan D and Coussens LM (2012). Accessories to the crime: functions of cells recruited to the tumor microenvironment. *Cancer Cell* **21**, 309–322.

[11] Hanahan D and Weinberg RA (2011). Hallmarks of cancer: the next generation. *Cell* **144**, 646–674.

[12] Brown JM and Koong AC (2008). High-dose single-fraction radiotherapy: exploiting a new biology? *Int J Radiat Oncol Biol Phys* **71**, 324–325.

[13] Barcellos-Hoff MH, Park C, and Wright EG (2005). Radiation and the microenvironment—tumorigenesis and therapy. *Nat Rev Cancer* **5**, 867–875.

[14] Golden EB, Pellicciotta I, Demaria S, Barcellos-Hoff MH, and Formenti SC (2012). The convergence of radiation and immunogenic cell death signaling pathways. *Front Oncol* **2**, 88.

[15] Schaue D, Xie MW, Ratikan JA, and McBride WH (2012). Regulatory T cells in radiotherapeutic responses. *Front Oncol* **2**, 90.

[16] Lugade AA, Moran JP, Gerber SA, Rose RC, Frelinger JG, and Lord EM (2005). Local radiation therapy of B16 melanoma tumors increases the generation of tumor antigen-specific effector cells that traffic to the tumor. *J Immunol* **174**, 7516–7523.

[17] Gupta A, Probst HC, Vuong V, Landshammer A, Muth S, Yagita H, Schwendener R, Pruschy M, Knuth A, and van den Broek M (2012). Radiotherapy promotes tumor-specific effector $CD8^+$ T cells via dendritic cell activation. *J Immunol* **189**, 558–566.

[18] Lee Y, Auh SL, Wang Y, Burnette B, Meng Y, Beckett M, Sharma R, Chin R, Tu T, Weichselbaum RR, et al. (2009). Therapeutic effects of ablative radiation on local tumor require $CD8^+$ T cells: changing strategies for cancer treatment. *Blood* **114**, 589–595.

[19] Paris F, Fuks Z, Kang A, Capodieci P, Juan G, Ehleiter D, Haimovitz-Friedman A, Cordon-Cardo C, and Kolesnick R (2001). Endothelial apoptosis as the primary lesion initiating intestinal radiation damage in mice. *Science* **293**, 293–297.

[20] Garcia-Barros M, Paris F, Cordon-Cardo C, Lyden D, Rafii S, Haimovitz-Friedman A, Fuks Z, and Kolesnick R (2003). Tumor response to radiotherapy regulated by endothelial cell apoptosis. *Science* **300**, 1155–1159.

[21] Bhowmick NA, Neilson EG, and Moses HL (2004). Stromal fibroblasts in cancer initiation and progression. *Nature* **432**, 332–337.

[22] Orimo A and Weinberg RA (2006). Stromal fibroblasts in cancer: a novel tumor-promoting cell type. *Cell Cycle* **5**, 1597–1601.

[23] Kalluri R and Zeisberg M (2006). Fibroblasts in cancer. *Nat Rev Cancer* **6**, 392–401.

[24] Bremnes RM, Donnem T, Al-Saad S, Al-Shibli K, Andersen S, Sirera R, Camps C, Marinez I, and Busund LT (2011). The role of tumor stroma in cancer progression and prognosis: emphasis on carcinoma-associated fibroblasts and non-small cell lung cancer. *J Thorac Oncol* **6**, 209–217.

[25] Orimo A, Gupta PB, Sgroi DC, Arenzana-Seisdedos F, Delaunay T, Naeem R, Carey VJ, Richardson AL, and Weinberg RA (2005). Stromal fibroblasts present in invasive human breast carcinomas promote tumor growth and angiogenesis through elevated SDF-1/CXCL12 secretion. *Cell* **121**, 335–348.

[26] Ksiazkiewicz M, Gottfried E, Kreutz M, Mack M, Hofstaedter F, and Kunz-Schughart LA (2010). Importance of CCL2-CCR2A/2B signaling for monocyte migration into spheroids of breast cancer-derived fibroblasts. *Immunobiology* **215**, 737–747.

[27] Gaggioli C, Hooper S, Hidalgo-Carcedo C, Grosse R, Marshall JF, Harrington K, and Sahai E (2007). Fibroblast-led collective invasion of carcinoma cells with differing roles for RhoGTPases in leading and following cells. *Nat Cell Biol* **9**, 1392–1400.

[28] Duda DG, Duyverman AM, Kohno M, Snuderl M, Steller EJ, Fukumura D, and Jain RK (2010). Malignant cells facilitate lung metastasis by bringing their own soil. *Proc Natl Acad Sci USA* **107**, 21677–21682.

[29] Barcellos-Hoff MH and Ravani SA (2000). Irradiated mammary gland stroma promotes the expression of tumorigenic potential by unirradiated epithelial cells. *Cancer Res* **60**, 1254–1260.

[30] Liu D and Hornsby PJ (2007). Senescent human fibroblasts increase the early growth of xenograft tumors via matrix metalloproteinase secretion. *Cancer Res* **67**, 3117–3126.

[31] Rodier F, Coppe JP, Patil CK, Hoeijmakers WA, Munoz DP, Raza SR, Freund A, Campeau E, Davalos AR, and Campisi J (2009). Persistent DNA damage signalling triggers senescence-associated inflammatory cytokine secretion. *Nat Cell Biol* **11**, 973–979.

[32] Wang W, Li Q, Yamada T, Matsumoto K, Matsumoto I, Oda M, Watanabe G, Kayano Y, Nishioka Y, Sone S, et al. (2009). Crosstalk to stromal fibroblasts induces resistance of lung cancer to epidermal growth factor receptor tyrosine kinase inhibitors. *Clin Cancer Res* **15**, 6630–6638.

[33] Mueller KL, Madden JM, Zoratti GL, Kuperwasser C, List K, and Boerner JL (2012). Fibroblast-secreted hepatocyte growth factor mediates epidermal growth factor receptor tyrosine kinase inhibitor resistance in triple-negative breast cancers through paracrine activation of Met. *Breast Cancer Res* **14**, R104.

[34] Straussman R, Morikawa T, Shee K, Barzily-Rokni M, Qian ZR, Du J, Davis A, Mongare MM, Gould J, Frederick DT, et al. (2012). Tumour micro-environment elicits innate resistance to RAF inhibitors through HGF secretion. *Nature* **487**, 500–504.

[35] Liu D and Hornsby PJ (2007). Fibroblast stimulation of blood vessel development and cancer cell invasion in a subrenal capsule xenograft model: stress-induced premature senescence does not increase effect. *Neoplasia* **9**, 418–426.

[36] Hellevik T, Pettersen I, Berg V, Winberg JO, Moe BT, Bartnes K, Paulssen RH, Busund LT, Bremnes R, Chalmers A, et al. (2012). Cancer-associated fibroblasts from human NSCLC survive ablative doses of radiation but their invasive capacity is reduced. *Radiat Oncol* **7**, 59.

[37] Park JE, Lenter MC, Zimmermann RN, Garin-Chesa P, Old LJ, and Rettig WJ (1999). Fibroblast activation protein, a dual specificity serine protease expressed in reactive human tumor stromal fibroblasts. *J Biol Chem* **274**, 36505–36512.

[38] de Jager W, te Velthuis H, Prakken BJ, Kuis W, and Rijkers GT (2003). Simultaneous detection of 15 human cytokines in a single sample of stimulated peripheral blood mononuclear cells. *Clin Diagn Lab Immunol* **10**, 133–139.

[39] Khan SS, Smith MS, Reda D, Suffredini AF, and McCoy JP Jr (2004). Multiplex bead array assays for detection of soluble cytokines: comparisons of sensitivity and quantitative values among kits from multiple manufacturers. *Cytometry B Clin Cytom* **61**, 35–39.

[40] Shevchenko A, Jensen ON, Podtelejnikov AV, Sagliocco F, Wilm M, Vorm O, Mortensen P, Boucherie H, and Mann M (1996). Linking genome and proteome by mass spectrometry: large-scale identification of yeast proteins from two dimensional gels. *Proc Natl Acad Sci USA* **93**, 14440–14445.

[41] Ishihama Y, Oda Y, Tabata T, Sato T, Nagasu T, Rappsilber J, and Mann M (2005). Exponentially modified protein abundance index (emPAI) for estimation of absolute protein amount in proteomics by the number of sequenced peptides per protein. *Mol Cell Proteomics* **4**, 1265–1272.

[42] Xing JZ, Zhu L, Gabos S, and Xie L (2006). Microelectronic cell sensor assay for detection of cytotoxicity and prediction of acute toxicity. *Toxicol In Vitro* **20**, 995–1004.

[43] Atienza JM, Yu N, Kirstein SL, Xi B, Wang X, Xu X, and Abassi YA (2006). Dynamic and label-free cell-based assays using the real-time cell electronic sensing system. *Assay Drug Dev Technol* **4**, 597–607.

[44] Abassi YA, Xi B, Zhang W, Ye P, Kirstein SL, Gaylord MR, Feinstein SC, Wang X, and Xu X (2009). Kinetic cell-based morphological screening: prediction of mechanism of compound action and off-target effects. *Chem Biol* **16**, 712–723.

[45] Eisenberg MC, Kim Y, Li R, Ackerman WE, Kniss DA, and Friedman A (2011). Mechanistic modeling of the effects of myoferlin on tumor cell invasion. *Proc Natl Acad Sci USA* **108**, 20078–20083.

[46] Arnaoutova I and Kleinman HK (2010). *In vitro* angiogenesis: endothelial cell tube formation on gelled basement membrane extract. *Nat Protoc* **5**, 628–635.

[47] West MD, Pereira-Smith OM, and Smith JR (1989). Replicative senescence of human skin fibroblasts correlates with a loss of regulation and overexpression of collagenase activity. *Exp Cell Res* **184**, 138–147.

[48] Suzuki M and Boothman DA (2008). Stress-induced premature senescence (SIPS)—influence of SIPS on radiotherapy. *J Radiat Res* **49**, 105–112.

[49] Lee AC, Fenster BE, Ito H, Takeda K, Bae NS, Hirai T, Yu ZX, Ferrans VJ, Howard BH, and Finkel T (1999). Ras proteins induce senescence by altering the intracellular levels of reactive oxygen species. *J Biol Chem* **274**, 7936–7940.

[50] Mishra P, Banerjee D, and Ben-Baruch A (2011). Chemokines at the crossroads of tumor-fibroblast interactions that promote malignancy. *J Leukoc Biol* **89**, 31–39.

[51] Erez N, Truitt M, Olson P, Arron ST, and Hanahan D (2010). Cancer-associated fibroblasts are activated in incipient neoplasia to orchestrate tumor-promoting inflammation in an NF-κB-dependent manner. *Cancer Cell* **17**, 135–147.

[52] Kuhlmann UC, Chwieralski CE, Reinhold D, Welte T, and Buhling F (2009). Radiation-induced matrix production of lung fibroblasts is regulated by interleukin-8. *Int J Radiat Biol* **85**, 138–143.

[53] Ohuchida K, Mizumoto K, Murakami M, Qian LW, Sato N, Nagai E, Matsumoto K, Nakamura T, and Tanaka M (2004). Radiation to stromal fibroblasts increases invasiveness of pancreatic cancer cells through tumor-stromal interactions. *Cancer Res* **64**, 3215–3222.

[54] Olson OC and Joyce JA (2012). Microenvironment-mediated resistance to anticancer therapies. *Cell Res* [E-pub ahead of print].

[55] Fuks Z, Persaud RS, Alfieri A, McLoughlin M, Ehleiter D, Schwartz JL, Seddon AP, Cordon-Cardo C, and Haimovitz-Friedman A (1994). Basic fibroblast growth factor protects endothelial cells against radiation-induced programmed cell death *in vitro* and *in vivo*. *Cancer Res* **54**, 2582–2590.

[56] Rades D, Setter C, Dahl O, Schild SE, and Noack F (2012). Fibroblast growth factor 2—a predictor of outcome for patients irradiated for stage II–III non-small-cell lung cancer. *Int J Radiat Oncol Biol Phys* **82**, 442–447.

[57] Wilson TR, Fridlyand J, Yan Y, Penuel E, Burton L, Chan E, Peng J, Lin E, Wang Y, Sosman J, et al. (2012). Widespread potential for growth-factor-driven resistance to anticancer kinase inhibitors. *Nature* **487**, 505–509.

[58] Takeuchi S, Wang W, Li Q, Yamada T, Kita K, Donev IS, Nakamura T, Matsumoto K, Shimizu E, Nishioka Y, et al. (2012). Dual inhibition of Met kinase and angiogenesis to overcome HGF-induced EGFR-TKI resistance in EGFR mutant lung cancer. *Am J Pathol* **181**, 1034–1043.

[59] Rendon BE, Willer SS, Zundel W, and Mitchell RA (2009). Mechanisms of macrophage migration inhibitory factor (MIF)-dependent tumor microenvironmental adaptation. *Exp Mol Pathol* **86**, 180–185.

[60] Capparelli C, Whitaker-Menezes D, Guido C, Balliet R, Pestell TG, Howell A, Sneddon S, Pestell RG, Martinez-Outschoorn U, Lisanti MP, et al. (2012). CTGF drives autophagy, glycolysis and senescence in cancer-associated fibroblasts via HIF1 activation, metabolically promoting tumor growth. *Cell Cycle* **11**, 2272–2284.

[61] Thijssen VL, Brandwijk RJ, Dings RP, and Griffioen AW (2004). Angiogenesis gene expression profiling in xenograft models to study cellular interactions. *Exp Cell Res* **299**, 286–293.

[62] Tseng D, Vasquez-Medrano DA, and Brown JM (2011). Targeting SDF-1/CXCR4 to inhibit tumour vasculature for treatment of glioblastomas. *Br J Cancer* **104**, 1805–1809.